Photocatalytic diphenhydramine degradation under different radiation sources: Kinetic studies and energetic comparison

N. López, P. Marco, J. Giménez[*], S. Esplugas

Department of Chemical Engineering and Analytical Chemistry, Faculty of Chemistry, Universitat de Barcelona, C/Martí i Franqués 1, 08028 Barcelona, Spain

ARTICLE INFO

ABSTRACT

The degradation of diphenhydramine hydrochloride (DPH) by TiO_2 photocatalysis was studied under different radiation sources: UVC, black blue lamps (BLB), simulated solar radiation (SB, Solarbox) and solar radiation (CPCs, Compound Parabolic Concentrators) at lab and pilot plant scales. Results indicated that photolysis showed an important role in the DPH abatement under UVC radiation (32.5% of DPH conversion), being negligible in all other cases. Different TiO_2 concentrations (0.05, 0.1 and 0.4 g/L) were used in SB device and the best results were obtained for 0.4 g/L: 35.7% of DPH conversion, after 60 min of irradiation. For comparison purposes, concentration of 0.4 g/L TiO_2 was used in all the devices. The best results obtained after 60 min of irradiation using only TiO_2 were 44.8% of DPH degradation in BLB and 9.0% of mineralization in SB. The addition of H_2O_2 improves the photocatalytic process (without H_2O_2) and the best results obtained were when UVC was used obtaining 100% DPH degradation and 28.6% TOC reduction. Concerning the removal efficiencies to the energy used, the best results were obtained for UVC with H_2O_2 (4492 mg DPH/kWh and 2246 ppm DPH/kWh), being also the corresponding cheapest costs (2.89×10^{-5} €/mg DPH and 5.79×10^{-5} €/ppm DPH). In terms of efficiency between 380 and 400 nm (absorption range for TiO_2), BLB presents the best results. Kinetic constants were also estimated referred to the irradiation time (h^{-1}) or the accumulated energy (kJ^{-1}), the highest values correspond to UVC with hydrogen peroxide ($7.64\,h^{-1}$ and $0.493\,kJ^{-1}$). Finally, toxicity and reaction intermediates were identified and DPH photo-degradation pathway was proposed.

1. Introduction

In the last years, water scarcity and quality have become a worldwide concern [1]. Every day large amounts of water are contaminated by different pollutants coming from domestic or industrial uses. Pollution of water, regulated by Directive (2013/39/EU) [2] as regards priority substances in the field of water policy, is generally decreasing. However, organic substances with harmful properties such as pharmaceuticals and personal care products are increasingly detected in the environment [3,4]. Spain is ranked as one of the world's largest consumer of pharmaceuticals [5]. These compounds are recalcitrant and with bioaccumulation problems [6–8]. They are also resistant to conventional wastewater treatments and are found in effluents at concentrations ranging 0.1–20.0 μg/L [9–11].

Among those pollutants, there is a special group of pharmaceuticals, antihistaminic drugs, easily found in waters. Between them, diphenhydramine hydrochloride (DPH) is the classic H_1 receptor antagonist used in pregnancy for the treatment of allergies and nausea, as well as an analgesic adjuvant in cancer pain. This kind of drugs can be achieved in wastewaters coming from some pharmaceutical industries in concentrations between 1300–1400 μg/L and some antibiotics can reach concentrations between 28,000–31,000 μg/L [12]. DPH has relatively low molecular weight and high lipid solubility, allowing easy blood–brain barrier and placental passage [13]. Unfortunately, information on the environmental fate and toxicity to aquatic species is scarce for most pharmaceuticals [14]. Due to the growing demand of society for the decontamination of water, regulations are increasingly strict in recent years, raising the research on methods to eliminate pharmaceuticals from water and wastewater, and this is the case of advanced oxidation processes (AOPs) [15,16].

AOPs are environmental friendly methods based on in situ production of hydroxyl radical (·OH) as main oxidant, which is able to react non-selectively with most organic compounds [17]. Different studies have been reported related to the photocatalytic treatment of DPH [18,19]. However, studies about DPH removal under different radiation sources and at low catalyst concentrations have not yet been reported.

The present work is focused on the degradation and mineralization

of DPH by photocatalytic treatment in different experimental devices. Experiments were performed in three laboratory scale photoreactors under artificial irradiation sources: UVC lamps (monochromatic radiation, maximum at 254 nm), black blue lamps (emission ranging from 300 to 410 nm, maximum at 365 nm) and simulated solar radiation (Solarbox with Xe lamp, spectrum similar to the solar one in the UV range). Moreover, a solar reactor has been used, at pilot plant scale, based on CPC configuration capable to collect the direct and diffuse radiation [20]. The energetic and economic efficiencies of the different tested devices were evaluated and compared. The most important intermediates have been also proposed.

2. Materials and experimental set-ups

2.1. Chemicals and reagents

The solution of 50 mg/L of DPH ($C_{17}H_{21}NO \cdot HCl$, HPLC grade, purity $\geq 98\%$ from Sigma-Aldrich) was prepared using deionized water. This high concentration (50 mg/L) was selected to assure accurate measurements of concentrations and to follow TOC. Moreover, this concentration was chosen to represent the conditions of wastewater coming from some pharmaceutical industries [21]. Acetonitrile (analytical reagent grade from Fischer Chemical) and orthophosporic acid (85% from Panreac Quimica) were used for HPLC analysis. H_2O_2 (30% w/w, from Merck), $NaHSO_3$ and MeOH (PAI from Panreac) reagents were used without further purification. Heterogeneous photocatalysis was performed using TiO_2 P-25 (Evonik, Germany).

2.2. Techniques and analytical instruments

DPH concentration was monitored by HPLC from Waters using a SEA18 Teknokroma column (250 × 4.6 mm i.d.; 5 μm particle size) and a Waters 996 photodiode array detector. The mobile phase was composed by water (pH 3) and acetonitrile (70:30), injected with a flowrate of 0.85 mL/min. DPH concentration was followed at UV maximum absorbance (220 nm). TOC was analyzed with a Shimadzu TOC-V CNS analyzer. H_2O_2 consumption was followed using the metavanadate spectrophotometric method at 450 nm [22]. H_2O_2 contained in samples was quenched with sodium hydrogen sulfite or the same volume of methanol, to avoid further reactions depending on the analysis to be done. For the intermediates identification, samples were analyzed by the electrospray ionization/mass spectrometry using an electrospray (ion spray) ESI–MS and a LC/MSD-TOF (Agilent Technologies) mass spectrometer. With the purpose to evaluate the acute toxicity depending of the different conditions Microtox® bioassays were performed. This method measures the inhibition of light emission of bioluminescent bacteria *vibrio fischeri* caused by the presence of toxic compounds in the aqueous media. All the tests were carried out in a Microtox® M500 toxicity analyzer (Modern Water, UK). All samples were filtered with a polyethersulfone membrane filter (0.45 μm, Chemlab) to remove the catalyst before analytical procedures.

2.3. Experimental devices

All the experimental devices described below have already been used in other investigations of the group and extensively described in other publications [23–25].

2.3.1. Artificial irradiation: UVC reactor

The experiments with UVC lamps were performed in a thermostatic Pyrex-jacketed 2 L vessel (inner diameter 11 cm, height 23 cm), equipped with three low pressure mercury lamps (Phillips TUV 8W, G8T5) located at the center of reactor. Lamps emit monochromatic radiation (254 nm). The effective radiation power was measured by ferrioxalate actinometry [26] and the obtained value was 4.31 J/s at 254 nm. A solution of DPH (50 mg/L) was introduced in the reactor

with TiO_2 (0.4 g/L), and immediately the lamps were switched on. Next H_2O_2 (15, 75 or 150 mg/L) was added depending on the experiment to be carried out. Magnetic stirring was used to ensure a good mixing. The temperature of the solution was maintained constant at 25 °C with the recirculated water by the jacket connected to an ultra-thermostatic bath (P Selecta).

2.3.2. Artificial irradiation: black blue lamps (BLB) reactor

BLB reactor consists on a 2 L Pyrex-jacketed thermostatic vessel (inner diameter 11 cm, height 23 cm), equipped with three 8 W BLB lamps (Philips TL 8W-08 FAM) located at the center of reactor. The radiative power was 1.55 J/s between 300 and 410 nm, measured by o-nitrobenzaldehyde actinometry [22]. The used actinometry changes according to the wavelength range of lamp emission. The tank was fed with DPH solution (50 mg/L) and TiO_2 (0.4 g/L). H_2O_2 (15, 75 or 150 mg/L) was added depending on the experiment to be carried out. The solution was maintained at constant temperature (25 °C) by controlling the jacket temperature with an ultra-thermostatic bath (P Selecta).

2.3.3. Artificial solar irradiation: Solarbox (SB)

A Solarbox (CO.FO.ME.GRA, 220V, 50 Hz) was used with a Xenon lamp (Phillips 1 kW), located at the top of the device. The effective radiation power was 0.97 J/s between 300 and 410 nm, measured also by o-nitrobenzaldehyde actinometry [22]. The tubular photoreactor (24 cm length, 2.11 cm diameter, Duran glass material) was placed at the bottom of the Solarbox on the axis of a parabolic mirror made of reflective aluminum. A filter cutting off wavelengths under 280 nm was placed between the lamp and the reactor. The DPH solution (50 mg/L) was prepared in a batch jacketed feeding tank (total volume 1L), connected to an ultra-thermostatic bath (Haake K10) to assure constant temperature during the process. H_2O_2 (15, 75 or 150 mg/L) and TiO_2 (0.05, 0.1, 0.4 g/L) were added depending on the experiment to be carried out. The solution to be treated was pumped to solarbox by a peristaltic pump (Ecoline VC-280 II, Ismatec) from the feeding tank with a flow-rate of 0.71 L/min. All connections employed were made of Teflon to avoid losses. A preliminary sample was collected before irradiation, representing initial concentration at time 0.

2.3.4. Solar irradiation: CPC reactor

Photocatalytic experiments were also carried out in a solar pilot plant based on compound parabolic collectors (CPC), at the University of Barcelona (latitude 41.4 N, longitude 2.1 W). The CPC consists in a module, 41° inclined, with a mirror made of polished aluminum, with 6 parallel tubular quartz reactors (length 56 cm, inner diameter 1.75 cm, wall thickness 0.15 cm). The total volume irradiated was 0.95 L. The total mirror's area for solar irradiation capture-reflection was 0.228 m². Experiments were done between 12:00 and 18:00 h in summer and temperature was 30 ± 5 °C. The exposure time was enough to reach the total hydrogen peroxide consumption. The aqueous suspension of DPH was pumped, with a peristaltic pump with a flow-rate 2.6 L/min, from the stirred (RW 16 basic agitator IKA) reservoir tank (5 L) to irradiated quartz tubes and continuously recirculated. The specific solar radiation was measured in each sample time ranging 12.45 W/m² to 49.78 W/m², by a spectroradiometer Bentham DMc300. The reservoir tank was fed with DPH solution (50 mg/L) and 0.4 g/L of TiO_2, with or without H_2O_2 (0 or 150 mg/L).

3. Results and discussions

DPH degradation by photocatalysis was evaluated during one hour based on previous experiments perfomed, in each experimental device. Different concentrations of H_2O_2 (15, 75 and 150 mg/L) and TiO_2 (0.05, 0.1 and 0.4 g/L) were used depending on the experiment to be carried out. These TiO_2 and H_2O_2 concentrations can be broadly found in literature and they were also selected based on the previous

experience [27–30].

In this section, degradation and mineralization results are shown with respect to the accumulated energy (Q_{acc}, kJ/L), which was calculated according Eq. (1) [22,31].

$$Q_{acc} = \sum_{i=0}^{n} \frac{I. \Delta t_i}{V} \qquad (1)$$

I is the incident photon flow (kJ/s), Δt_i is the time interval (s) and V is the volume of the treated solution (L).

Preliminary tests were performed to study the DPH adsorption onto the catalyst surface. Different DPH concentrations (0, 12.5, 25, 50, 75 and 100 mg/L) were prepared with 0.4 g TiO$_2$/L, at natural pH (6.2), constant stirring and temperature (25 °C $\pm$ 0.5) under dark conditions. A two-parameter Langmuir isotherm model was tested in the fitting of adsorption data (Eq. (2)).

$$q_e = \frac{q_m K_a C_e}{1 + K_a C_e} \qquad (2)$$

q_e (mol/g) is the DPH amount adsorbed on the catalyst, C_e (mg/L) is the DPH concentration in solution after adsorption, K_a is the Langmuir adsorption equilibrium constant and q_m represents the maximum monolayer adsorption capacity. In our case, the obtained values fot K_a and q_m where 0.017 L/mol and 0.048 mol/g, respectively. These low values of K_a and q_m show that adsorption does not play an important role.

To evaluate the temperature influence, 1 L of DPH solution with a concentration of 200 mg/L was placed in the stirred tank and heated at 20, 40, 60 and 80 °C. Degradation and/or mineralization were not observed at any tested temperature.

DPH degradation by photolysis was studied and experiments were carried out with 50 mg/L of DPH in the different reactors without catalyst. The influence of photolysis on DPH degradation and mineralization is low in Solarbox (60 min, Q_{acc} = 3.5 kJ/L between 300 and 410 nm), CPC (60 min, Q_{acc} = 2.28 kJ/L between 315 and 400 nm) and BLB (60 min, Q_{acc} = 2.79 kJ/L between 300 and 410 nm), the results were 2.5, 1.4 and 4.7% of DPH degradation, respectively. Only UVC light (60 min, Q_{acc} = 7.76 kJ/L at 254 nm), achieving 32.5% of DPH removal in 60 min, is powerful enough to break the DPH bonds, because UVC covers the range of light absorption of DPH (λ_{max} at 220 nm). Fig. 1 summarizes the obtained results. Moreover, photolysis did not promote relevant mineralization (4.5% for BLB).

3.1. SB reactor

In SB, DPH elimination was (60 min, Q_{acc} = 3.5 kJ/L between 300 and 410 nm): 35.7% (for 0.4 g/L TiO$_2$), 27.0% (for 0.1 g/L TiO$_2$) and 15.8% (for 0.05 g/L TiO$_2$). TOC removal is low and catalyst
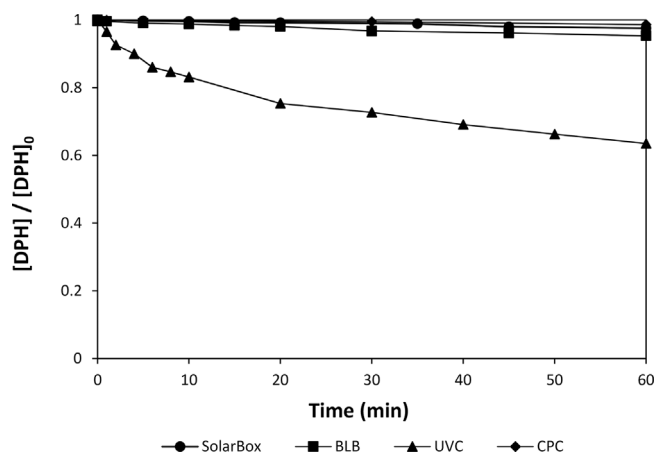
concentration does not significantly influence. Catalyst load can improve DPH conversion. However, catalyst settling was observed for concentrations higher than 0.4 g/L TiO$_2$ in SB, decreasing the reaction rate by radiation scattering and catalyst losses. The optimal loading depends on the photoreactor geometry and operation conditions [19].

The effect of H$_2$O$_2$ addition was evaluated, with 0.4 g/L of catalyst and 50 mg/L DPH, in SB, BLB, UVC and CPC reactors. In SB, BLB and UVC three amounts of H$_2$O$_2$ (15, 75 or 150 mg/L) were added directly in the feeding tank. In CPC only 150 mg/L of H$_2$O$_2$ were used. In SB the highest degradation of DPH was obtained with 150 mg/L of H$_2$O$_2$ (62.6%). The joint presence of UV, H$_2$O$_2$ and TiO$_2$ improves DPH degradation. Several articles have also reviewed that the addition of external oxidants such as hydrogen peroxide, in this case, during the photocatalytic process can improve the degradation of the organic matter when they are added in suitable dose [32,33]. H$_2$O$_2$ is considered to have two functions in the photocatalytic oxidation. It accepts a photogenerated electron from the conduction band of the semiconductor to form ·OH radicals (Reaction (3)). In addition, it forms ·OH radicals according to Reaction (4) [34,35].

$$H_2O_2 + e^- \rightarrow °OH + OH^- \qquad (3)$$

$$H_2O_2 + °O_2^- \rightarrow °OH + OH^- + O_2 \qquad (4)$$
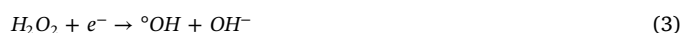
Moreover, as reported in different articles and pointed out in Reaction (3), H$_2$O$_2$ is an electron acceptor having a high activity and efficiency in this role than oxygen for the titania conduction-band electrons [36,37]. However, mineralization levels in SB were low: 9.0%, 9.8%, 10.7% and 16.3% TOC conversion for 0, 15, 75 or 150 mg/L of H$_2$O$_2$, respectively. Fig. 2 shows the results of DPH conversion and mineralization vs. the accumulated energy (Q_{acc}, kJ/L) between 300 and 410 nm for different H$_2$O$_2$ concentrations.

3.2. CPC reactor

Fig. 3 shows the obtained results of DPH conversion and mineralization vs. the accumulated energy (Q_{acc}, kJ/L) in CPCs.

As commented in the Section 3.1 and for the same reasons, the addition of hydrogen peroxide improves the DPH degradation, as seen in Fig. 3 (360 min, Q_{acc} = 36 kJ/L between 315 and 400 nm, 0.4 g/L TiO$_2$): 49.2% (without H$_2$O$_2$) and 69.5% (150 mg/L H$_2$O$_2$). However, the TOC removal rate (11.2% without H$_2$O$_2$ and 13.7% with H$_2$O$_2$) has not significant improvement. For comparison with the other experimental devices, the DPH degradation, at 60 min of irradiation, was 8.7% (without H$_2$O$_2$) and 53.8% (with 150 mg/L H$_2$O$_2$), while the TOC conversion was 5.6% and 6.7%, without H$_2$O$_2$ or with 150 mg/L H$_2$O$_2$, respectively.

Fig. 1. DPH degradation by photolysis in all experimental devices.

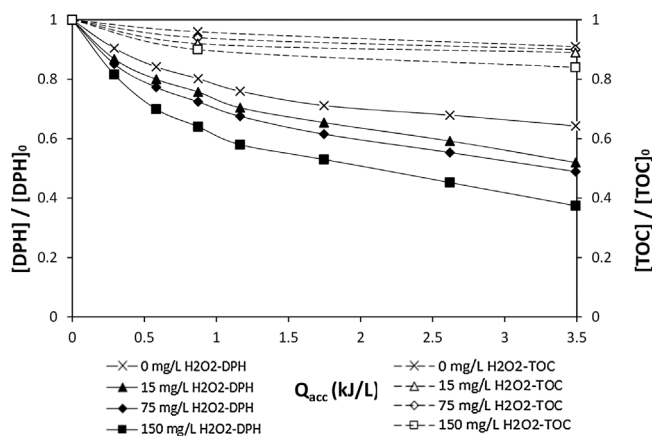**Fig. 2.** DPH conversion and TOC removal in SB reactor for different H$_2$O$_2$ concentrations at 60 min. [TiO$_2$] = 0.4 g/L.
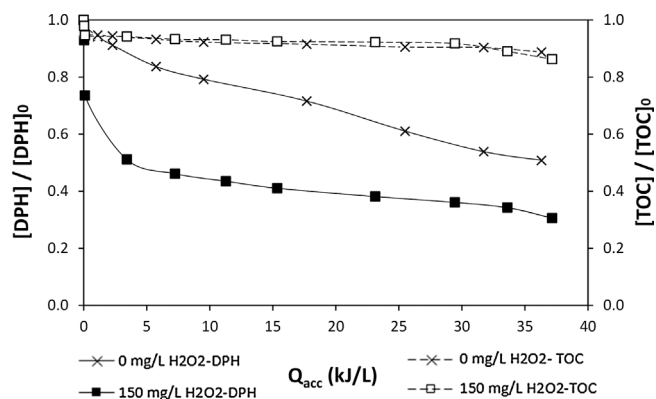
Fig. 3. DPH conversion and TOC removal in CPC reactor at 360 min, $[TiO_2]$ = 0.4 g/L.
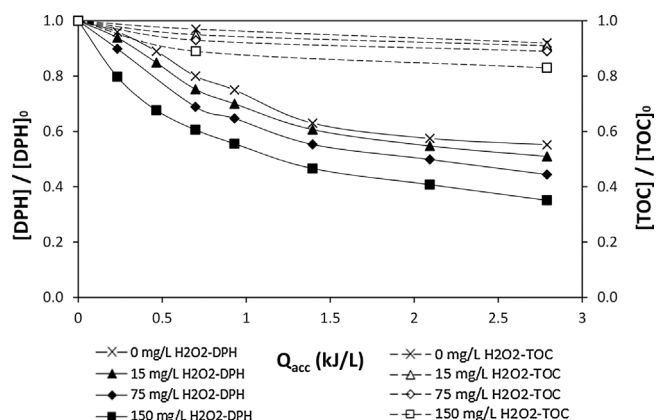

Fig. 4. DPH conversion and TOC removal in BLB reactor at 60 min, $[TiO_2]$ = 0.4 g/L.

3.3. BLB reactor

Fig. 4 shows the results of DPH conversion and mineralization vs. the accumulated energy (Q_{acc}, kJ/L) for different H_2O_2 concentrations, in BLB reactor.

DPH elimination was (60 min, Q_{acc} = 2.79 kJ/L between 300 and 410 nm, 0.4 g/L TiO_2): 44.8% (without H_2O_2), 49.0% (15 mg/L H_2O_2), 55.6% (75 mg/L H_2O_2) and 64.9% (150 mg/L H_2O_2). The obtained results show that with 15 mg/L of H_2O_2 the DPH elimination is not much higher, as it happens in SB. In BLB reactor only 4.2% more of degradation was achieved with 15 mg/L H_2O_2. In the presence of high dose of hydrogen peroxide (150 mg/L H_2O_2) this degradation increases. However, the degradation values do not increase more than 50% in BLB, SB and CPC, due to absorption wavelength (254 nm) of hydrogen peroxide, as commented in Section 3.4. As in the other tested experimental devices, peroxide acts as additional source of hydroxyl radicals improving the overall efficiency, as commented in Section 3.1. Mineralization levels in this system were low too: 8.1%, 9.2%, 10.0% and 17.3% with 0, 15, 75 and 150 mg/L of H_2O_2, respectively.

3.4. UVC reactor

In UVC reactor (Fig. 5), DPH elimination was (60 min, Q_{acc} = 7.76 kJ/L at 254 nm, 0.4 g/L TiO_2): 32.5% (without H_2O_2), 55.7% (15 mg/L H_2O_2), 79.7% (75 mg/L H_2O_2) and 100.0% (150 mg/L H_2O_2). As observed in the results in the presence with hydrogen peroxide the degradation of DPH increases a 23.2% with minimum dose (15 mg/L H_2O_2). Moreover, total DPH degradation was reached when 150 mg/L of H_2O_2 were employed. Thus, in this reactor is observed much better the effect of hydrogen peroxide addition, because the lamps emit at 254 nm and H_2O_2 absorbs at this wavelength. Again, the joint presence of UV, H_2O_2 and TiO_2 improves DPH degradation.
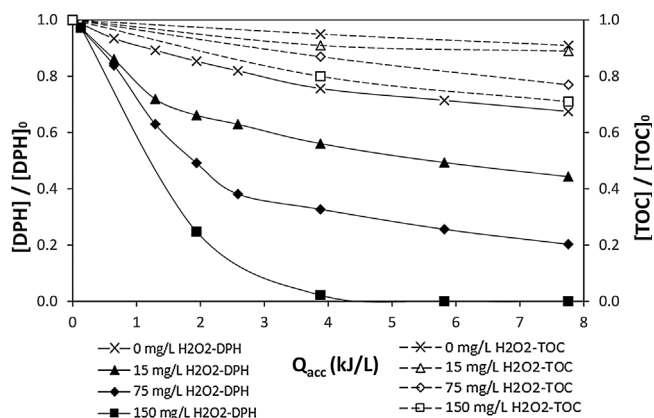

Fig. 5. DPH conversion and TOC removal in UVC reactor at 60 min, $[TiO_2]$ = 0.4 g/L.

Moreover, not only UV/TiO_2/H_2O_2 process acts, but also UV/H_2O_2 was deeding, which amplifies the effects of the hydrogen peroxide manifested by Reactions (3) and (4) in Section 3.1. Mineralization levels (without H_2O_2 or with 15 mg/L H_2O_2) were low too, but using 75 mg/L and 150 mg/L of H_2O_2 were achieved higher levels than for other conditions and reactor. TOC conversion was 8.7% (without H_2O_2), 10.6% (with 15 mg/L H_2O_2), 23.3% (with 75 mg/L H_2O_2) and 28.6% (with 150 mg/L H_2O_2).

3.5. Energetic comparison of photocatalytic process in SB, BLB, UVC and CPC reactors

As beforehand observed, DPH removal and mineralization was evaluated in four different experimental devices: a solar CPC pilot plant reactor, a solar simulator reactor (SB), a three black light lamps based reactor (BLB) and a three UVC lamps based reactor. For comparison, the selected experimental conditions were the same in all devices, differing only in the geometry of the reactors and wavelength and radiation power. Energetic comparisons were performed to evaluate the efficiencies (in DPH removal) referred to the lamp power or referred to the energy associated to the wavelength range where TiO_2 absorbs (380–400 nm). The total efficiency for an experiment was calculated in each device considering concentration (ppm/kWh) (Eq. (5)) or the total treated volume (mg/kWh) (Eq. (6)). To determine kWh referred to the lamp power it was used the nominal power of each lamp multiplied by the hours of experiment. The lamp power was 0.024 kWh for BLB and UVC reactors and 1 kWh for SB. The energy (kWh) associated to the wavelength range where TiO_2 absorbs was determined by using actinometries in each reactor. To assess the total cost for an experiment the inverse values of efficiency were multiplied by the medium value of the electricity cost in Spain (0.13 €/kWh). Efficiency and cost were evaluated for both DPH conversion and TOC removal at 60 min, as Table 1 shows. Of course, for the evaluation of the global efficiency or global costs, other parameters have to be considered such cost of installations, reactives analysis, and so one [38,39]. Here, only efficiencies referred to energy source were considered for a quick and first approximation to the problem.

$$\frac{(ppm_{initial} - ppm_{final})}{kWh} \quad (5)$$

$$\frac{(ppm_{initial} - ppm_{final})}{kWh} \times Volume \quad (6)$$

In terms of lamp efficiency without H_2O_2, BLB presents the best results in all cases, followed by UVC with similar results (see Table 1). It can also be observed that the use of hydrogen peroxide improves the efficiency in all cases (two times in the case of BLB and SB and four times in the case of UVC), probably due to the photolysis of H_2O_2 itself and the generation of more hydroxyl radicals. With H_2O_2, UVC device

Table 1
Costs, lamp efficiency and efficiency between 380 and 400 nm at time 60 min. Kinetic constants are also presented.

			BLB	UVC	SB	CPC
Lamp efficiency at time 60 min						
0.4 g/L TiO_2	Efficiency	(mg DPH/kWh)	1588	1373	17.6	–
		(mg TOC/kWh)	248	259	3.3	–
		(ppm DPH/kWh)	794	687	17.6	–
		(ppm TOC/kWh)	124	130	3.3	–
	Cost	(€/mg DPH)	8.18×10^{-5}	9.47×10^{-5}	7.38×10^{-3}	–
		(€/mg TOC)	5.02×10^{-4}	5.02×10^{-4}	0.04	–
		(€/ppm DPH)	1.64×10^{-4}	1.89×10^{-4}	7.38×10^{-3}	–
		(€/ppm TOC)	1.05×10^{-3}	1.00×10^{-3}	0.04	–
0.4 g/L TiO_2 150 mg/L H_2O_2	Efficiency	(mg DPH/kWh)	2830	4492	32.2	–
		(mg TOC/kWh)	452	868	6.0	–
		(ppm DPH/kWh)	1415	2246	32.2	–
		(ppm TOC/kWh)	226	434	6.0	–
	Cost	(€/mg DPH)	4.59×10^{-5}	2.89×10^{-5}	4.03×10^{-3}	–
		(€/mg TOC)	2.88×10^{-4}	1.49×10^{-4}	0.02	–
		(€/ppm DPH)	9.19×10^{-5}	5.79×10^{-5}	4.03×10^{-3}	–
		(€/ppm TOC)	5.75×10^{-4}	2.99×10^{-4}	0.02	–
Efficiency at time 60 min between 380 and 400 nm						
0.4 g/L TiO_2	Efficiency	(mg DPH/kWh)	135,220	–	65,222	25,474
		(mg TOC/kWh)	21,141	–	12,222	14,889
		(ppm DPH/kWh)	67,610	–	65,222	5095
		(ppm TOC/kWh)	10,571	–	12,222	2978
	Cost	(€/mg DPH)	9.61×10^{-7}	–	1.99×10^{-6}	–
		(€/mg TOC)	6.15×10^{-6}	–	1.06×10^{-5}	–
		(€/ppm DPH)	1.92×10^{-6}	–	1.99×10^{-6}	–
		(€/ppm TOC)	1.23×10^{-5}	–	1.06×10^{-5}	–

	BLB	UVC	SB	CPC
Kinetic constants (h^{-1})				
0.4 g/L TiO_2	0.594	0.393	0.425	0.092
0.4 g/L TiO_2 − 150 mg/L H_2O_2	1.047	7.643	0.984	0.774
Kinetic constants (kJ^{-1})				
0.4 g/L TiO_2	0.107	0.025	0.122	0.008
0.4 g/L TiO_2 − 150 mg/L H_2O_2	0.188	0.493	0.282	0.021

shows the best results. SB presents the worse results, due to the use of a lamp with 1 kW power whereas that UVC and BLB use lamps with 24 W power. The reasons for the observed differences in DPH abatement can be related, obviously, to the geometry of devices and the radiation used. The influence of radiation source is especially clear in the case of UVC that becomes the best device when H_2O_2 is added to the reaction medium. This fact is due to the photolysis of hydrogen peroxide favored in the UVC range (as commented before), increasing the amount of hydroxyl radicals present in the medium and favoring the DPH degradation. In addition, the geometry of the reactor used in UVC and BLB favors the light improvement because lamps are located at the center of the cylindrical reactor. All these reasons can explain that UVC and BLB offer best results than SB in DPH abatement.
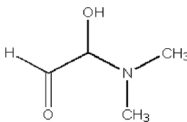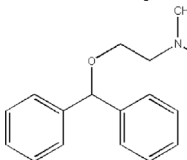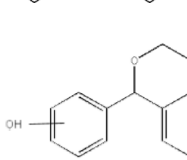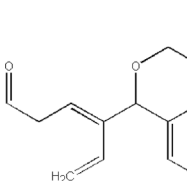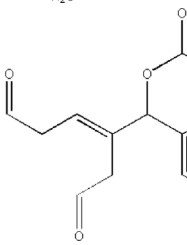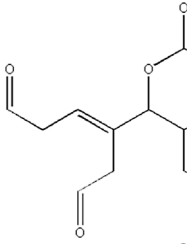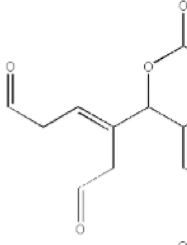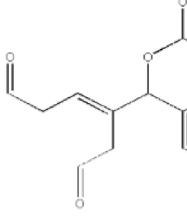
Other parameter interesting to evaluate is the efficiency referred to the range of absorption for TiO_2, that is 380–400 nm. The energy corresponding to this interval has been calculated from the radiation entering the photoreactors evaluated by actinometries, as explained in Section 2. In this case, the efficiency for UVC lamp cannot be calculated, because UVC does not emit at 380–400 nm and the effect of TiO_2 is minimal. For similar reasons, the experiments with hydrogen peroxide were not considered because the extra hydroxyl radicals generated from H_2O_2 are produced out of the wavelength range considered (380–400 nm). For the rest of tested devices, as observed in Table 1, it is difficult to establish a general trend. When ppm reduction is considered, BLB and SB present similar efficiencies and higher than CPC probably because the percentage of radiation entering the photoreactor in the considered range (380–400 nm) is higher for BLB and SB. However, if the reaction volume is taken into account and, therefore, the efficiency is calculated with respect to the treated mg, the device showing clearly the best results is BLB. This fact points out the importance of scaling when efficiencies are considered, that means treated

volume plays an important role when the efficiency of a process is evaluated. The efficiency of the CPC is a further example in this sense, since, taking into account the total volume treated, its efficiency in demineralization (mg TOC/kWh) is lower than that obtained for BLB but even slightly higher than that obtained for SB (14,889, 21,141 and 12,222 for CPC, BLB and SB, respectively). Thus, the volume treated in CPCs is large than in the other devices and this fact can imply an effect of scaling up with the showed improvement of efficiency.

A draft economical comparison was performed to evaluate the costs for DPH removing in each experimental device. As a first approximation, only the costs related to the radiation source were considered, because these costs can highlight the importance of well choosing the radiation source in carrying out an AOP. Obviously, solar natural radiation based reactors (CPC) do not present costs in terms of electricity of lamps. When all the power of the lamps is considered and H_2O_2 is not used, BLB device shows the lowest costs and UVC shows slightly higher costs, although considering the efficiency in TOC decrease, the costs are practically the same (see Table 1). The great difference obviously appears when estimating the costs for SB that are much higher due to the power difference of the lamps used, 1 kW for SB and 24 W for BLB and UVC. When H_2O_2 is used, things change and UVC happens to be the cheapest device with costs that are practically half of those corresponding to BLB. SB remains the most expensive for the reasons noted above (1 kW of lamp power versus 24 W of the other two). The change in trend with hydrogen peroxide can also be explained by that already mentioned above, when discussing the efficiencies, related to the increase of the photolysis of hydrogen peroxide by the use of UVC radiation, favoring the generation of more hydroxyl radicals, with the consequent increase of efficiency and costs reduction from an energetic point of view.

When only the energy consumption in range between 380 and

Table 2
DPH and its main intermediates detected by LC/MS analysis in photodegradation experiments.

m/z (Da)	Rt [min]	Elemental composition	Proposed structure (Label)	Experimental conditions	
				With H_2O_2	Without H_2O_2
104 (m+1)	1.70	$C_4H_9NO_2$	DPH-104	√	√
256 (m+1)	2.50	$C_{17}H_{21}NO$	DPH-256	√	√
272 (m+1)	2.25	$C_{17}H_{21}NO_2$	DPH-272	√	√
274 (m+1)	1.94	$C_{17}H_{23}NO_2$	DPH-274	√	√
290 (m+1)	2.04	$C_{17}H_{23}NO_3$	DPH-290	√	√
306 (m+1)	1.84	$C_{17}H_{23}NO_4$	DPH-306	√	
322 (m+1)	1.85	$C_{17}H_{23}NO_5$	DPH-322	√	
338 (m+1)	1.86	$C_{17}H_{23}NO_6$	DPH-338	√	
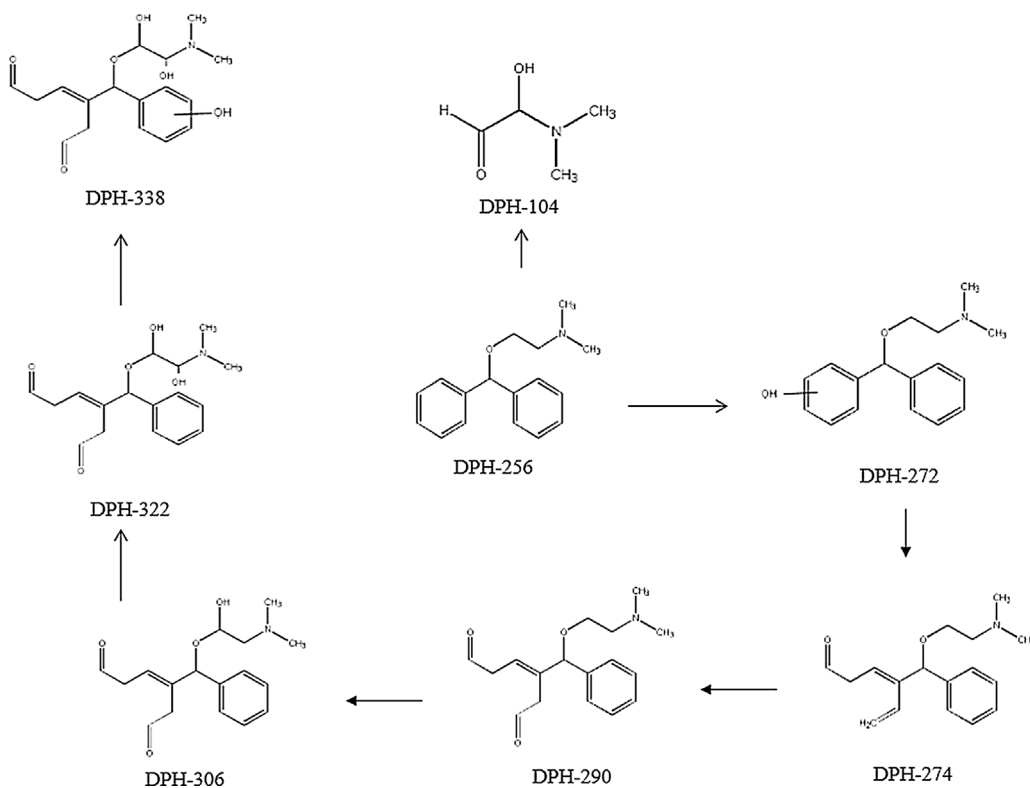
400 nm is considered, UVC and CPC are not included for the reasons explained before. Thus, the comparison between BLB and SB shows that costs are similar, as observed in Table 1. The large differences observed, when the entire power lamp was considered, disappear because in this case only the radiation useful for titania absorption is considered.

Concerning the reaction kinetics, kinetic constants were obtained from the graphics ln [DPH]/[DPH$_0$] vs accumulated energy (kJ) or vs irradiation time, at 60 min of irradiation for all the cases. For the calculation of kinetic constants, the accumulated energy includes the treated volume and, for this reason, the units are kJ. The accumulated energy was used because radiation plays an important role in photocatalytic processes, influencing in a decisive manner on the reaction rate. Thus, if only time is considered and the radiation entering the reactors is omitted, we can arrive to a misinterpretation of the results. The accumulated energy is the energy entering the photoreactor during all the experiment time and was measured by actinometries, as explained, in Section 2, except in the case of CPC where radiation was measured by radiometers. The catalyst concentration was 0.4 g/L in all the cases.

As shown in Table 1, when time fittings are considered (without H$_2$O$_2$), CPC shows the low kinetic constant (h^{-1}) and BLB the best ones; however, UVC and SB present results very close to BLB. When hydrogen peroxide was added, UVC gives the best results and BLB, SB and CPC show similar results. The best results for UVC can be again related to the photolysis of hydrogen peroxide by the UVC light and the increase of hydroxyl radicals in the reaction medium, increasing the reaction rate.

If kinetics is referred to accumulated radiation instead time, the kinetic constants (kJ^{-1}) show the highest values for SB and BLB (0.122 and 0.107, respectively, see Table 1). UVC shows a value four times lower (0.025) and CPC gives the poor value (0.008). This behavior can be expected from the data observed in Figs. 2–5, where CPC needs highest amount of radiation to obtain conversion similar to that obtained for the other devices. When hydrogen peroxide is added to reaction medium, UVC presents the highest value for the kinetic constant (0.493 kJ^{-1}). This behavior is the same observed for all the tested

parameters, already commented, and is related to the increase of hydroxyl radicals due to the photolysis of H$_2$O$_2$ in the UVC range. In this case, SB (0.282 kJ^{-1}) shows results slightly better than BLB (0.188 kJ^{-1}), being again CPC giving the low kinetic constant (0.021 kJ^{-1}).

All the results commented in this section point out the influence of radiation and reactor geometry on the reaction rate and consequently on the pollutant degradation. The importance of taking into account radiation instead of time, when calculating the kinetic constants, has also been shown. Finally, it is also clear that, when comparisons are made, it is necessary to indicate clearly how they have been done. Thus, it has been shown that it is not the same to evaluate the efficiency in the degradation of the pollutant per kWh taking into account the absolute amount degraded (ppm) or also taking into account the treated reaction volume (mg). Moreover, it is necessary to specify clearly how the radiation efficiency is calculated: radiation emitted by the lamp, radiation that can absorb the catalyst, etc.

3.6. Toxicity, intermediates and degradation pathways

Regarding to hazardousness of treated solutions, toxicity (*vibrio fisheri*) was assessed for the different experimental conditions in all devices. This includes experiments without H$_2$O$_2$ and experiments with H$_2$O$_2$ (15, 75, 150 mg/L). The *vibrio fisheri* test indicated that DPH was initially non-toxic. However, after performing the experiments on the different experimental devices, the test was repeated to verify that the intermediates that could be generated were also non-toxic. In fact, it was verified in all cases that the tests of *vibrio fisheri* indicate that final solutions were non-toxic.

Intermediates identification was performed with samples taken at 60 min of irradiation in all the devices, with all experimental conditions. The intermediates identified are shown in Table 2. These intermediates were the same under the different radiation sources and different experimental devices tested and no significant difference was observed when the concentrations of H$_2$O$_2$ were varied.

According to the intermediates found and their proposed structures,

pathways can be proposed (Fig. 6).

The photocatalytic process lets to the formation of m/z 104, m/z 272 and m/z 274 (DPH 104, DPH-272 and DPH-274). Formation of DPH-104 could be by cleavage of DPH-256 and subsequently hydroxylation of two carbons and oxidation of one of them. Meanwhile, DPH-272 could be formed from DPH-256 by the hydroxylation of the molecule. Furthermore, due to OH· generation, it is logical to expect the addition of OH· on the aromatic ring and to open the aromatic ring leading to the formation of DPH-274. Moreover, the hydroxylation form of DPH-274 could be attacked by OH· forming a compound (DPH-290). In the same way, when the hydrogen peroxide was added DPH-306, DPH-322 and DPH-338 were formed. This is due to the formation of more OH· when there is more addition of peroxide. Thus, it is logical that these compounds are formed [40]. In addition, the low mineralization observed in all the cases agrees the proposed reaction pathway. Summarizing, from the reaction intermediates that could be detected, it appears that the oxidation processes occur mainly through the hydroxyl radicals, as indicated in Fig. 6 and, therefore, it seemed that the other mechanisms had a secondary role. It also seems very likely that molecular oxygen will act as an electron acceptor by giving the radical superoxide anion ($\cdot O_2 -$) [34], but in turn it reacts rapidly with hydrogen peroxide to give hydroxyl radicals (see Reaction (4) in Section 3.1) reinforcing the role of hydroxyl radicals.

4. Conclusions

The four devices tested (UVC, BLB, SB and CPC) are useful for DPH degradation by TiO_2 photocatalysis, obtaining the best results in BLB (44.8% DPH degradation). However, mineralization is very low in all the cases. In the case of UVC system, the DPH and TOC removals are due mainly to photolysis. In this way, results improve when H_2O_2 was added and the best results were obtained in UVC with 100% of DPH degradation, being the mineralization 28.6%. This improvement can be explained by the photolysis of hydrogen peroxide in UVC system, increasing the generation of hydroxyl radicals and, therefore, the reaction rate. Considering the efficiency referred to lamp power, BLB (without H_2O_2) and UVC (with H_2O_2) show the highest efficiencies (mg DPH/kWh and ppm DPH/kWh) in the photocatalytic treatment of DPH. This behavior agrees with the observation that UVC gives the highest kinetic (kJ^{-1}) constant and the highest conversion because the power of lamp promotes also the photolysis of H_2O_2 increasing the presence of hydroxyl radicals and, consequently, the reaction rate. Concerning the costs (€/mg DPH or €/ppm DPH) the observed trends are the same, SB presents the worst results respect to the lamp efficiency due to the highest lamp power (1000 W for SB and 24 W for BLB and UVC). In terms of efficiency in the absorption range of TiO_2 (380–400 nm), BLB presents the best results in DPH degradation, followed by SB and CPC. Toxicity studies pointed out that DPH can be considered non-toxic and neither its intermediates. The intermediates obtained in the photocatalytic treatment of DPH show, on the one hand, that the breakdown of the DPH molecule and subsequent hydroxylation of the molecule proceeds; while, on the other hand, they also indicate that hydroxylations occur on the DPH molecule because of the hydroxyl radicals generated.

Acknowledgments

References

[1] N. Miranda-García, M. Ignacio Maldonado, J.M. Coronado, S. Malato, Degradation study of 15 emerging contaminants at low concentration by immobilized TiO_2 in a pilot plant, Catal. Today 151 (2010) 107–113.

[2] European Commission Joint Research Centre, Directive 2013/39/EU of the European Parlimnet and of the Council amending Directives 2000/60/EC and 2008/105/EC as regards priority substances in the field of water policy. Part I. EUR 2011/429 EN, Eur. Chem. Bur. Part II (2013) 226/1–226/17.

[3] J. Munthe, E. Brorström-Lundén, M. Rahmberg, L. Posthuma, R. Altenburguer, W. Brack, D. Bunke, G. Engelen, B.M. Gawlick, J. Van Gils, D. López Herráez, T. Rydberg, J. Slobodnik, A. Van Wezel, An expended conceptual framework for solution-focused management of chemical pollution in European waters, Environ. Sci. Eur. 29 (1) (2017) 13.

[4] D.J. Lapwortha, N. Baranb, M.E. Stuarta, R.S. Warda, Review emerging organic contaminants in groundwater: a review of sources, fate and occurrence, Environ. Pollut. 163 (2012) 287–303.

[5] S. Alonso, M. Catalá, R. Maroto, Pollution by psychoactive pharmaceuticals in the Rivers of Madrid metropolitan area (Spain), Environ. Int. 36 (2010) 195–201.

[6] N. Miranda, S. Miranda, I.M. Maldonado, S. Malato, B. Sánchez, Regeneration approaches for TiO_2 immobilized photocatalyst used in the elimination of emerging contaminants in water, Catal. Today 230 (2014) 27–34.

[7] S.D. Richardson, Environmental mass spectrometry: emerging contaminants and current issues, Anal. Chem. 80 (12) (2008) 4373–4402.

[8] B. Kasprzyk-Hordern, R.M. Dinsdale, A.J. Guwy, The occurrence of pharmaceuticals, personal care products, endocrine disruptors and illicit drugs in surface water in South Wales, UK, Water Res. 42 (13) (2008) 3498–3518.

[9] A. De Luca, R.F. Dantas, S. Esplugas, Assessment of iron chelates efficiency for photo-Fenton at neutral pH, Water Res. 61 (2014) 232–242.

[10] Z. Yimeng, C. Wenhai, X. Ting, Y. Daqiag, Y. Bin, L. Pan, A. Na, Impact of pre-oxidation using H_2O_2 and ultraviolet/H_2O_2 on desinfection byproducts generated from chlor(am)ination of chloramphenicol, Chem. Eng. J. 317 (2017) 112–118.

[11] B.I. Escher, R. Baumgartner, M. Koller, K. Treller, J. Linert, C.D. McCardell, Environmental toxicology and risk assessment of pharmaceuticals from hospital wastewater, Water Res. 45 (2011) 75–92.

[12] D.G. Joakim Larrson, C. De Pedro, N. Paxeus, Effluent from drug manufactures contains extremely high levels of pharmaceuticals, J. Hazard. Mater. 148 (2007) 751–755.

[13] A. Moraes, A. Schwarz, H. Spinosa, Maternal exposure to diphenhydramine during the fetal period in rats: effects on physical and neurobehavioral development and on neurochemical parameters, Neurotoxicol. Teratol. 26 (2004) 681–692.

[14] V. Roos, L. Gunnarsson, J. Fick, Prioritising pharmaceuticals for environmental risk assessment: towards adequate and feasible first-tier selection, Sci. Total Environ. 421–422 (2012) 102–110.

[15] B. Ning, N. Graham, Y.P. Zhang, M. Nakonechny, M.G. El Din, Degradation of endocrine disrupting chemicals by ozone/AOPS, Ozone: Sci. Eng. 29 (2007) 153–176.

[16] N. De la Cruz, J. Giménez, S. Esplugas, D. Granjean, L.F. De Alencastro, C. Pulgarín, Degradation of 32 emergent contaminants by UV and neutral photo-fenton in domestic wastewater effluent previously treated by activated sludge, Water Res. 45 (6) (2012) 1947–1957.

[17] I. Sirés, E. Brillas, Remediation of water pollution caused by pharmaceutical residues based on electrochemical separation and degradation technologies: a review, Environ. Int. 40 (2012) 212–229.

[18] R.A.R. Monteiro, S.M. Miranda, V.J.P. Vilar, L.L. Pastrana-Martínez, P.B. Tavares, R.A.R. Boaventura, J.L. Faria, E. Pinto, A.M.T. Silva, N-modified TiO_2 photocatalytic activity towards diphenhydramine degradation and *Escherichia coli* inactivation in aqueous solutions, Appl. Catal. B: Environ. 162 (2015) 66–74.

[19] L.M. Pastrana-Martínez, J.L. Faria, J.M. Doña-Rodríguez, C. Fernández-Rodríguez, A.M.T. Silva, Degradation of diphenhydramine pharmaceutical in aqueous solutions by using two highly active TiO_2 photocatalyst: operating paramenters and photocatalytic mechanism, Appl. Catal. B: Environ. 113–114 (2012) 221–227.

[20] S. Malato, P. Fernández-Ibáñez, M.I. Maldonado, I. Oller, M.I. Polo-López, Solar photocatalytic pilot plants: commercially available reactors, in: Pierre Pichat (Ed.), Photocatalysis and Water Purification, Wiley-VCH, Weinheeim-Germany, 2013, pp. 377–397.

[21] D.G. Joakim Larrsson, C. De Pedro, N. Paxeus, Effluent from drug manufactures contains extremely high levels pf pharmaceuticals, J. Hazard. Mater. 148 (2007) 751–755.

[22] N. De la Cruz, V. Romero, R.F. Dantas, P. Marco, B. Bayarri, J. Giménez, S. Esplugas, O-Nitrobenzaldehydeactinometry in the presence of suspended TiO_2 for photocatalytic reactors, Catal. Today 209 (2013) 209–214.

[23] N. De la Cruz, R.F. Dantas, J. Giménez, S. Esplugas, Photolysis and TiO2 photocatalysis of the pharmaceutical propranolol: solar and artificial light, Appl. Catal. B-Environ. 130–131 (2013) 249–256.

[24] V. Romero, F. Méndez-Arriaga, P. Marco, J. Giménez, S. Esplugas, Comparing the photocatalytic oxidation of Metoprolol in a solarbox and a solar pilot plant reactor, Chem. Eng. J. 254 (2014) 17–29.

[25] V. Romero, Degradation of Metoprolol by Means of Advanced Oxidation Processes, Doctoral Thesis, University of Barcelona, 2015, http://hdl.handle.net/2445/65724.

[26] H.J. Kuhn, S.E. Braslavsky, R. Schmidt, Chemical actinometry (IUPAC technical report), Pure Appl. Chem. 76 (2004) 2105–2146.

[27] V. Romero, D. De la Cruz, R.F. Dantas, P. Marco, J. Giménez, S. Esplugas, Photocatalytic treatment of metoprolol and propranolol, Catal. Today 161 (2011) 115–120.

[28] V. Romero, P. Marco, J. Giménez, S. Esplugas, Adsorption and photocatalytic decomposition of the -blocker metoprolol in aqueous titanium dioxide suspensions: kinetics, intermediates, and degradation pathways, Int. J. Photoenergy (2013) 1–10.

[29] V. Romero, O. González, B. Bayarri, P. Marco, J. Giménez, S. Esplugas, Performance of different advanced oxidation technologies for the abatement of the beta-blocker metoprolol, Catal. Today 240 (2015) 86–92.

[30] V. Romero, O. González, B. Bayarri, P. Marco, J. Giménez, S. Esplugas, Degradation of Metoprolol by photo-Fenton: comparison of different photoreactors performance, Chem. Eng. J. 283 (2016) 639–648.

[31] P. Fernández, J. Blanco, C. Sichel, S. Malato, Water desinfection by solar photocatalysis using compound parabolic colectors, Catal. Today 101 (2005) 345–352.

[32] F.J. Beltrán, F.J. Rivas, R. Montero-de-Espinosa, Catalytic ozonation of oxalic acid in aqueous TiO_2 slurry reactor, Appl. Catal. B: Environ. 39 (2002) 221.

[33] S.G. De Moraes, R.S. Freire, N. Duran, Degradation and toxicity reduction of textile effluent by combined photocatalytic and ozonation processes, Chemosphere 40 (2000) 369.

[34] E.S. Elmolla, M. Chaudhuri, Photocatalytic degradation of amoxicillin, ampicillin and cloxacillin antibiotics in aqueous solution using UV/TiO_2 and $UV/H_2O_2/TiO_2$ photocatalysis, Desalination 252 (2010) 46–52.

[35] M. Kositzi, A. Antoniadis, I. Poulios, I. Kiridis, S. Malato, Solar photocatalytic treatment of simulated dyestuff effluents, Sol. Energy 77 (2004) 591–600.

[36] Z. Wang, C.S. Hong, Effect of hydrogen peroxide, periodate and persulfate on photocatalysis of 2-clorobiphenyl in aqueous TiO_2 suspensions, Water Res. 33 (1999) 2031.

[37] J. Fernández, J. Kiwi, J. Baeza, J. Freer, C. Lizama, H.D. Mansilla, Orange II photocatalysis on immobilized TiO_2 Effect of the pH and H_2O_2, Appl. Catal. B: Environ. 48 (2004) 205–211.

[38] J. Giménez, B. Bayarri, O. González, S. Malato, J. Peral, S. Esplugas, Advanced oxidation processes at laboratory scale: environmental and economic impacts, Sustain. Chem. Eng. 3 (2015) 3188–3196.

[39] D. Haranaka Funai, F. Didier, J. Giménez, P. Marco, S. Esplugas, A. Machulek Junior, Photocatalytic treatment of valproic acid sodium salt with TiO_2 in different experimental devices: an economic and energetic comparison, Chem. Eng. J. 327 (2017) 656–665.

[40] L.M. Pastrana-Martínez, N. Pereira, R. Lima, J.L. Faria, H.T. Gomez, A.M.T. Silva, Degradation of diphenhydramine by photo-Fenton using magnetically recoverable iron oxide nanoparticles as catalyst, Chem. Eng. J. 261 (2015) 45–52.